

Article

Surface-Initiated Polymerization with an Initiator Gradient: A Monte Carlo Simulation

Zhining Huang ¹, Caixia Gu ¹, Jiahao Li ¹, Peng Xiang ¹, Yanda Liao ², Bang-Ping Jiang ¹, Shichen Ji ^{1,3,*} 
and Xing-Can Shen ^{1,*}

¹ State Key Laboratory for Chemistry and Molecular Engineering of Medicinal Resources, Key Laboratory for Chemistry and Molecular Engineering of Medicinal Resources, Ministry of Education of China, Collaborative Innovation Center for Guangxi Ethnic Medicine, School of Chemistry and Pharmaceutical Sciences, Guangxi Normal University, Guilin 541004, China; huang_z_n@stu.gxnu.edu.cn (Z.H.); jiangbangping@mailbox.gxnu.edu.cn (B.-P.J.)

² School of Computer Science and Engineering & School of Software, Guangxi Normal University, Guilin 541004, China; lyd@gxnu.edu.cn

³ State Key Laboratory of Molecular Engineering of Polymers, Fudan University, Shanghai 200433, China

* Correspondence: shichen.ji@mailbox.gxnu.edu.cn (S.J.); xcshen@mailbox.gxnu.edu.cn (X.-C.S.)

Abstract: Due to the difficulty of accurately characterizing properties such as the molecular weight (M_n) and grafting density (σ) of gradient brushes (GBs), these properties are traditionally assumed to be uniform in space to simplify analysis. Applying a stochastic reaction model (SRM) developed for heterogeneous polymerizations, we explored surface-initiated polymerizations (SIPs) with initiator gradients in lattice Monte Carlo simulations to examine this assumption. An initial exploration of SIPs with ‘homogeneously’ distributed initiators revealed that increasing σ slows down the polymerization process, resulting in polymers with lower molecular weight and larger dispersity (D) for a given reaction time. In SIPs with an initiator gradient, we observed that the properties of the polymers are position-dependent, with lower M_n and larger D in regions of higher σ , indicating the non-uniform properties of polymers in GBs. The results reveal a significant deviation in the scaling behavior of brush height with σ compared to experimental data and theoretical predictions, and this deviation is attributed to the non-uniform M_n and D .

Keywords: gradient brush; surface-initiated polymerization; stochastic reaction model; Monte Carlo simulation



Citation: Huang, Z.; Gu, C.; Li, J.; Xiang, P.; Liao, Y.; Jiang, B.-P.; Ji, S.; Shen, X.-C. Surface-Initiated Polymerization with an Initiator Gradient: A Monte Carlo Simulation. *Polymers* **2024**, *16*, 1203. <https://doi.org/10.3390/polym16091203>

Academic Editors: Alexey V. Lyulin and Valeriy V. Ginzburg

Received: 21 March 2024

Revised: 22 April 2024

Accepted: 23 April 2024

Published: 25 April 2024



Copyright: © 2024 by the authors. Licensee MDPI, Basel, Switzerland. This article is an open access article distributed under the terms and conditions of the Creative Commons Attribution (CC BY) license (<https://creativecommons.org/licenses/by/4.0/>).

1. Introduction

Gradient brushes (GBs) are polymer brushes wherein properties, such as molecular weight, grafting density, or chemical composition, gradually vary in one or more directions along the substrate. GBs are powerful tools for high-throughput and low-cost investigations in the areas of physics, chemistry, biomaterials science, and biology [1–8]. In a single sample, a given surface parameter across a wide range can be systematically explored, avoiding the need for lengthy repetitive procedures and enhancing the efficiency of research and development [8]. Additionally, GBs are widely used to study interfacial phenomena like the directional transport of liquids, cell adhesion, and migration [9,10].

Surface-initiated polymerization (SIP) is a promising approach to synthesizing GBs with higher grafting density. There are two major forms of SIP classified by initiator distribution [3,11]: one with a homogeneous distribution of initiators and another with a gradient distribution. In the former case, GBs are obtained by controlling the spatial polymerization time, for example, using a movable mask or reaction solution, or by adjusting the spatial polymerization rate through methods such as varying the intensity of transmitted light with a filter in photopolymerization [12–16]. In the latter case, initiators with a gradient density are firstly anchored to the surface using methods such as the silane diffusion

method, nanolithography methods, or methods involving gradients of temperature or electrochemical potential [15–21]. Subsequently, SIP is carried out to yield GBs. Generally, the former is a simpler and more feasible method, while the latter is suitable for small-sized patterns and arbitrary structures [3].

Despite significant progress in the preparation of GBs, characterizing crucial properties such as grafting density (σ), molecular weight (M_n), and molecular weight distribution remains a challenging task [13,22,23]. The characterization of σ and M_n is interrelated since

$$\sigma = h\rho N_A / M_n, \quad (1)$$

where h is the height of a brush in the dry state, ρ is the density of a polymer, and N_A is Avogadro's constant. Gel permeation chromatography (GPC) is the most common method for directly determining the molecular weight of grafted polymers, involving the degrafting of polymer chains from a substrate. However, the GPC method requires a sufficient amount of a sample, posing a challenge for SIP, especially regarding polymerization on a flat substrate [2]. On the other hand, the accuracy of indirect measurement, achieved by incorporating sacrificial initiators for simultaneous bulk- and surface-initiated polymerizations and characterizing the resulting polymers in solution, has been a topic of debate [22,23]. Notably, neither direct nor indirect GPC methods offer insights into the spatial distribution of these properties in GBs.

The lack of information on molecular weight and grafting density has significantly hindered efforts toward comprehensively understanding gradient polymer brushes and applying them. An early study examined the scaling behavior between brush height and grafting density for a gradient polymer brush [17]. In this study, a polyacrylamide (PAAm) brush with a grafting density gradient was obtained via atom-transfer radical polymerization (ATRP) with an initiator gradient generated via the silane diffusion method [17,24]. Due to the absence of information on molecular weight, two assumptions were made to determine the grafting density in space: (1) the molecular weight of polymers along the substrate in GBs is uniform, and (2) there is similarity in the molecular weight between polymers in the GBs and those obtained in solution polymerization under the same conditions. Upon determining the dry brush height using variable-angle spectroscopic ellipsometry, the spatial distribution of grafting density was obtained using Equation (1). Subsequently, we examined the scaling relationship between the wet height of the brush and grafting density, revealing only a slight deviation from the theoretical prediction [17].

Although researchers have recognized the limitations of the uniform molecular weight assumption [17], it remains prevalent in experimental studies due to its simplicity. This raises a question: what is the significance of the effect of this assumption?

To answer this question, the polymerization mechanism should be examined, as it strongly influences properties such as molecular weight and dispersity. Computer simulations have played an important role in revealing the mechanisms of SIPs. A pioneering study was performed by Genzer using a Monte Carlo (MC) simulation [25], and it inspired studies using different simulation methods [26–35]. Typically, SIPs result in polymers with larger dispersity and smaller molecular weight compared to those generated via bulk-initiated polymerizations (BIPs). This trend holds even in simultaneous bulk- and surface-initiated polymerization [26,28,35]. Moreover, grafting density is a key parameter in SIP, impacting both the kinetics of the reaction and the properties of the polymers, such as molecular weight and dispersity. The main reason is that SIP is a heterogeneous polymerization, as the homogeneous distribution of free monomers is altered by the newly formed polymer brush [34], while BIP is a homogeneous polymerization.

According to the existing simulations of SIPs, it is natural to expect that the molecular weight should be non-uniform in an SIP with an initiator gradient. However, the significance of this difference in molecular weight and its potential impact on the scaling behavior observed in Ref. [17] remain uncertain because no simulations, to the best of our knowledge, have directly addressed this issue.

To address this gap, we conducted a lattice Monte Carlo simulation to examine SIP with initiator gradients (referred to as gradient polymerization in the remainder of this paper), using a stochastic reaction model (SRM) developed for heterogeneous polymerizations [34–36]. We explored two systems: one with a series of homogeneous SIPs with varying grafting densities, wherein the initiators were homogeneously distributed, and the other with SIPs with an initiator gradient. In both systems, the properties of the polymers are significantly affected by grafting density. Notably, the scaling relationship between the brush height and grafting density in GBs, as obtained in the simulation, diverges from the experimental results, highlighting the need for a more in-depth exploration of gradient polymerization. The lattice MC model and SRM algorithms are introduced in Section 2, while the results of living polymerizations with homogeneous and gradient initiators are shown in Section 3. Brief conclusions are provided in Section 4.

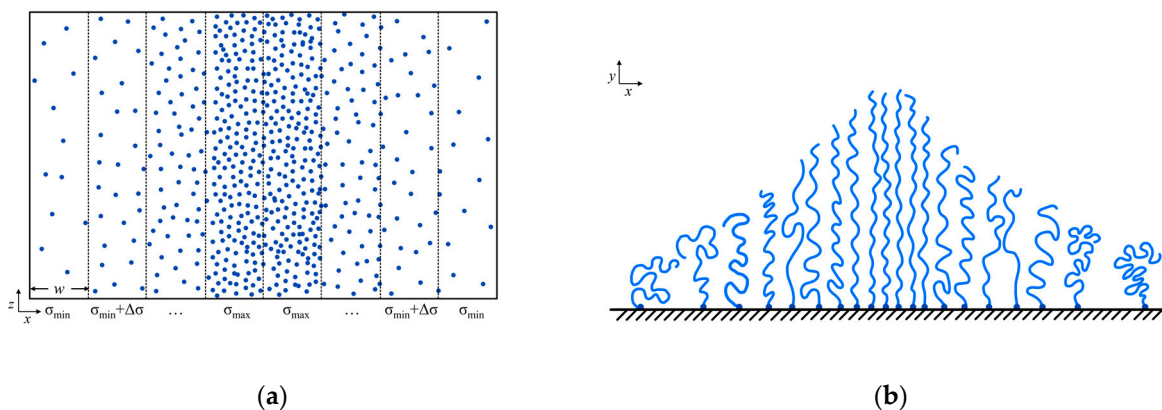
2. Models and Simulation Methods

2.1. Lattice Monte Carlo Simulation

In this study, we employed the Larson-type bond fluctuation model [37,38], which was previously utilized in our investigations of SIP and the flow behavior of polymer brushes [34–36,39]. Briefly, the simulation was carried out in a simple cubic lattice with a volume, V , equal to $L_x \times L_y \times L_z$. Each lattice site can be occupied by a monomer or initiator only once, and the bond length was set to 1 or $\sqrt{2}$. During relaxation, a monomer is randomly selected to be exchanged with one of its 18 nearest or next-nearest neighbor sites. This exchange will be accepted under the conditions that the neighbor site is vacant and that the exchange would not break the chain and cause bond intersection (possible bond intersections are shown in Figure S1). The excluded volume effect and entanglement were well considered in this model. The simulation time was measured in units of Monte Carlo steps (MCs), defined as all monomers attempting to move once, on average.

Two impenetrable walls were set in the $y = 1$ and L_y planes, respectively, while periodic boundary conditions were applied in both the x and z directions. In this simulation, the x direction represents the initiator gradient direction, the y direction indicates the chain growth direction, and the z direction corresponds to the equivalent direction. In the beginning, all the free monomers were randomly distributed in the system. The immobilized initiators were randomly positioned on the $y = 1$ plane during the investigation of homogeneous SIP. It should be noted that the term ‘homogeneous’ does not imply a perfectly ‘regular’ distribution of initiators, as shown in Figure S2. The properties of these two systems show subtle differences [30]. Instead, “homogeneous” is used in comparison to the gradient polymerization.

While studying gradient polymerization, the $y = 1$ plane was divided into multiple stripes in the x direction (initiator gradient direction), as illustrated in Scheme 1. Each stripe has a width w , resulting in a total number of L_x/w stripes. In the left part of the simulation box, the grafting density of the leftmost stripe is σ_{\min} and gradually increases with the value of $\Delta\sigma$ (the difference in density between successive stripes) with an increasing number of stripe locations until it reaches the maximum grafting density σ_{\max} . The grafting density in the right part mirrored that of the left part, i.e., the grafting density decreased from the middle to the rightmost stripe as the location of stripes shifted forward further. Within each stripe, the number of initiators can be calculated as $\sigma(x) \times w \times L_z$, with $\sigma(x)$ denoting the grafting density of a stripe, and these initiators exhibited a random distribution within the stripes.



Scheme 1. An illustration of the gradient distribution of initiators in the $y = 1$ plane (a) and the projection of gradient polymer brush in the xy direction (b). In this simulation, the x direction represents the initiator gradient direction, the y direction indicates the chain growth direction, and the z direction indicates the equivalent direction.

2.2. Implementation of Polymerization

In this study, a living polymerization was considered, which occurred at intervals of every τ MCs during the relaxation process. Here, τ is defined as the characteristic delay time, or reaction interval time [27,34–36,40]. By decreasing or increasing the value of τ , the reaction can be adjusted to make it diffusion-limited or reaction-limited.

The stochastic reaction model (SRM) proposed by our group was applied to model the polymerization [34–36]. Firstly, an initiator or active center was randomly selected. Then, the number of free monomers m within the radius of $\sqrt{2}$ was determined. The initiator or active center tries to react with a random monomer among these m free monomers with a given probability P_r , which is determined by the local number of free monomers and calculated as mP_0 (where P_0 is a constant representing the elementary reaction probability between one active center and one free monomer). If the reaction is accepted, the free monomer transforms into an active center for future reactions. Since P_r is determined by the local reaction environment, each active center reacts with its own probability. Thus, our SRM model fully accounts for the heterogeneous reaction microenvironment, which is the inherent character of SIP [34–36]. As demonstrated by living bulk-initiated polymerization, the polymerization kinetics obtained by this SRM were found to be very consistent with the theoretical predictions [34,36].

3. Results and Discussion

3.1. Homogeneous Surface-Initiated Polymerization

We first investigated a series of homogeneous SIPs with varying grafting densities and compared the properties at the same polymerization times. The parameters were fixed and set as follows: the dimensions of the simulation box were $L_x \times L_y \times L_z = 50 \times 77 \times 50$, the initial concentration of free monomers was $[M]_0 = 0.4$ monomers per lattice, the reaction interval time was $\tau = 10$ MCs, the simulation time was 2×10^6 MCs, and the elementary reaction probability was $P_0 = 0.001$. The results were averaged over 60 independent runs.

Figure 1a shows the number-average molecular weight M_n during polymerization with a given grafting density σ . It is evident that σ significantly influences the polymerization kinetics, with M_n increasing more rapidly at lower σ compared to higher values. Figure 1b shows M_n as a function of σ with a given polymerization time t . When σ is very low, M_n is nearly constant. However, when σ is high, M_n exhibits a monotonic decrease with an increasing σ . The decrease in M_n with increasing σ is related to the polymerization time. For example, when $t = 400,000$ MCs, the values of M_n are 21.7 and 13.5 at $\sigma = 0.1$ and 0.4, respectively. The latter ($M_n = 13.5$) is only about 62% of the former, and by $t = 800,000$ MCs, this ratio further decreases to 54%. Besides M_n , the dispersity ($D = M_w/M_n$) and molecular weight distribution (MWD) are also influenced by σ . The

dispersity increases with increasing σ (Figure 1c), and MWD becomes broader and more asymmetric (Figure 1d).

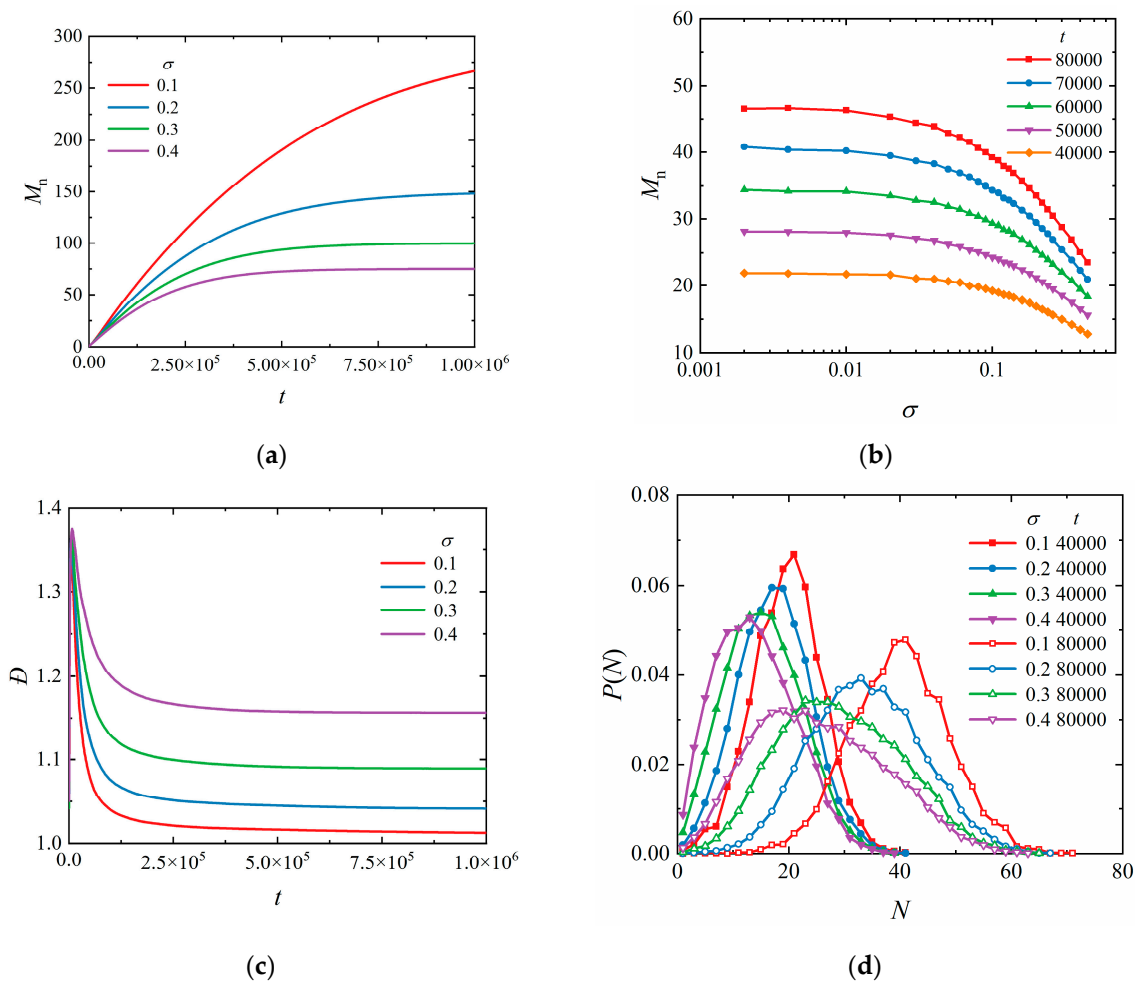


Figure 1. Influence of grafting density σ on surface-initiated polymerization with a homogeneous distribution of initiators. (a) Number-average molecular weight M_n as a function of polymerization time t with a given σ . The molecular weight with $\sigma = 0.1$ was saturated at the end of the simulation (2×10^6 MCs). (b) M_n as a function of σ with a given t . (c) Dispersity (D) as a function of t . (d) The molecular weight distribution $P(N)$ with a given σ .

The results suggest that in SIP, systems with different values of σ exhibit variations in polymer properties at the same polymerization time, preliminarily indicating that the molecular weight in GBs might be non-uniform due to the initiator gradient. It should be pointed out that molecular weight is independent of the concentration of initiators in living BIPs with low monomer conversion, and this can be proved as follows. The monomer conversion C of BIP can be written as

$$C = 1 - \frac{[M]_t}{[M]_0} = 1 - \exp(-(m_{\max} - 1)[I]_0 P_0 t / \tau), \tag{2}$$

where $[M]_t$ is the concentration of free monomers at time t , $[I]_0$ is the concentration of the initiator, and m_{\max} is the maximum number of free monomers around an active center, equal to 18 in this simulation. At low conversion, M_n linearly increases with t as

$$M_n = \frac{[M]_0 C}{[I]_0} \approx [M]_0 (m_{\max} - 1) P_0 t / \tau. \tag{3}$$

Thus, in BIP, molecular weight is only determined by reaction time, and it is independent of the number of initiators.

Why does this assumption hold for BIP but not SIP? The reason is that Equation (1) was deduced from a homogeneous polymerization system, such as BIP. However, SIP is a heterogeneous system, especially when σ is high. When σ is low, the active centers are far apart and react with free monomers like isolated active centers, resembling a homogeneous polymerization system. Conversely, when σ is large, brush-like polymers are obtained, and the system is no longer homogeneous as free monomers are expelled by the nascent polymers from the surface. The active centers near the surface react in an environment with a lower concentration of free monomers compared with those far from the surface. Such a heterogeneous reaction environment is the key feature of SIP, and the heterogeneity of the reaction environment increases with σ [34,35].

3.2. Surface-Initiated Polymerization with Initiator Gradient

We further investigated the gradient polymerization with a simulation box for which $L_x \times L_y \times L_z = 288 \times 72 \times 100$. The initial concentration of free monomers was $[M]_0 = 0.4$ monomers per lattice. As shown in Scheme 1, the grafting plane was divided into stripes with a width $w = 4$. In this study, the maximum grafting density of a stripe is $\sigma_{\max} = 0.42$, and the minimum is $\sigma_{\min} = 0.07$. We did not explore lower grafting densities as our primary interest lay in the scaling behavior of polymer brushes within regions with high grafting density. The difference in grafting density between the adjacent stripes is $\Delta\sigma = 0.01$. The corresponding steepness of the gradient is $\delta = \Delta\sigma/w = 0.0025$. As discussed later, such a steepness is low enough to examine the gradient polymerization process. Polymerization stops when the number-average molecular weight of the brush reaches 50. Such a molecular weight is large enough to ensure the system stays in the brush region; meanwhile, it can avoid the situation wherein some very long chains might approach the $y = L_y$ plane.

The density contour map (Figure 2a) clearly confirms the formation of a gradient brush. In the vertical direction, the polymer density decreases with an increasing distance from the surface. Horizontally, there is a gradient increase in the density from the low-grafting region ($x = 1$) to the high-grafting region ($x = 144$), which then decreases upon further shifting the x position forward. Meanwhile, the density contour map of free monomers exhibits the opposite trend (Figure 2b).

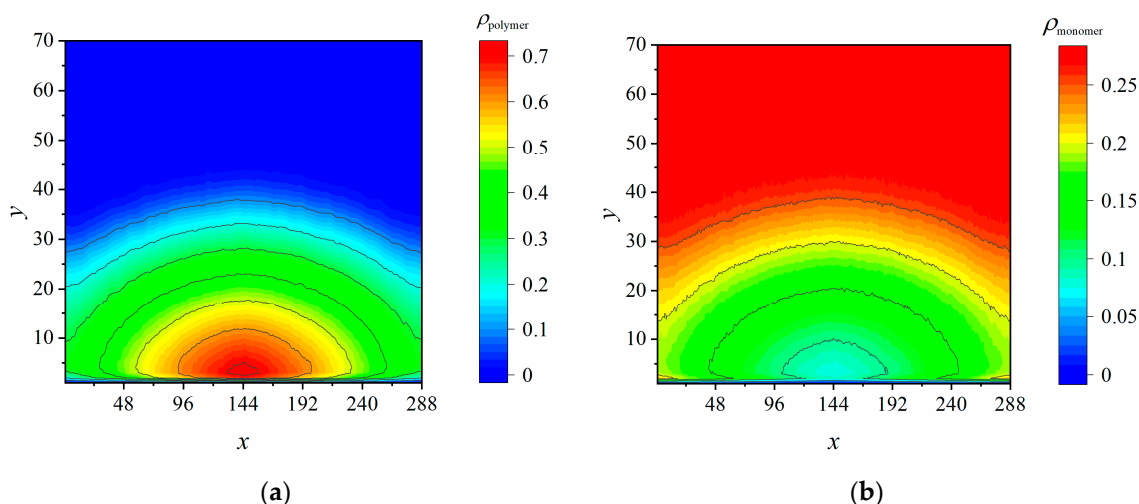


Figure 2. The density contour maps of polymer brush (a) and free monomers (b) in the gradient polymerization. The number-average molecular weight in the system is $M_n = 50$.

The molecular weights of the polymers at each stripe were examined (Figure 3a), with the results clearly proving that there is a non-uniform molecular weight in GBs. M_n decreases from the low-grafting regions (outsides) to the high-grafting regions (middle).

Although the overall M_n of the system is 50, it is only 42.4 in the middle, contrasting with the higher value of 65.5 on the outside areas. Such a notable difference in M_n should not be overlooked. We further compared the molecular weight and dispersity in gradient polymerization with those in SIP at the same reaction time (Figure 3b). The variation in M_n between different grafting density positions in gradient polymerization is smaller than that in SIP. This might be attributed to the competition among different polymerization regions in gradient polymerization. Higher-grafting-density regions tend to consume more monomers during the reaction. The dispersity of polymers in gradient polymerization increases with grafting density, which is similar to the trend observed in SIP (Figure 3b).

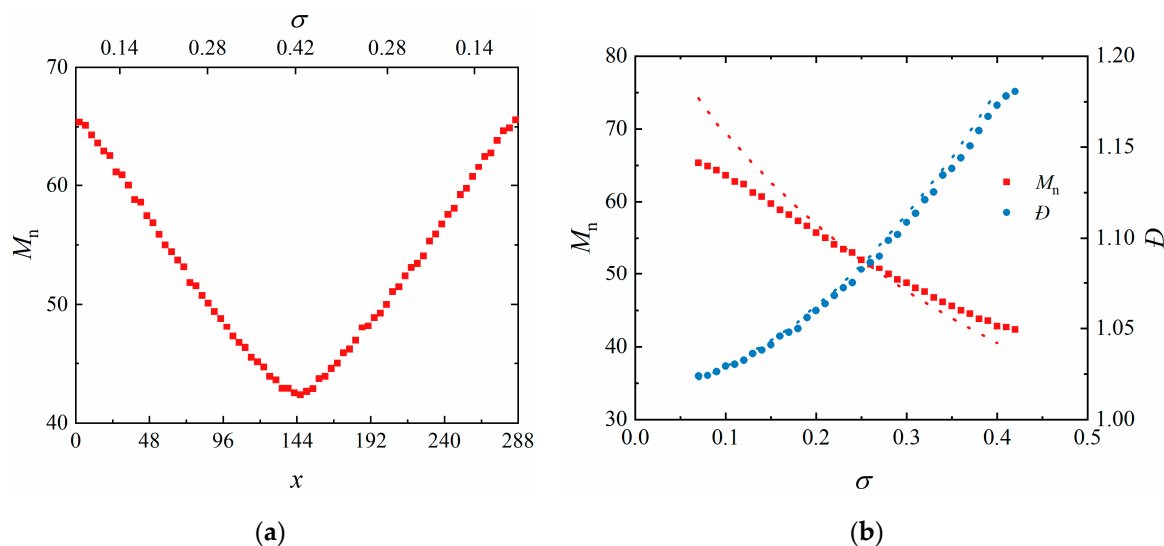


Figure 3. (a) M_n as a function of positions and corresponding grafting densities in gradient polymerization when the overall M_n of the system is 50. (b) M_n and D as a function of σ in both gradient polymerization (solid symbols) and SIP (dotted lines).

In experiments, the height of a brush in the dry state is widely used to estimate grafting density in accordance with Equation (1). In this study, we have supposed that the brush shown in Figure 2a vertically collapses onto the surface; thus, the dry height at position x , denoted as $h(x)$, can be calculated as follows:

$$h(x) = \sum_{y=1}^{L_y} \rho(x, y). \quad (4)$$

Figure 4a suggests that a gradient brush is obtained but that the dry height $h(x)$ does not linearly increase with the grafting density $\sigma(x)$, as depicted by Equation (1). This deviation from a linear relationship is evidently caused by the variations in M_n at different positions, as shown in Figure 3a. After normalizing the height with respect to the corresponding molecular weight, a linear relationship between $h(x)$ and $\sigma(x)$ can be restored.

The height in solution H is a key property of a polymer brush and is calculated as follows:

$$H(x) = \frac{\sum_{y=1}^{L_y} y\rho(x, y)}{\sum_{y=1}^{L_y} \rho(x, y)} \quad (5)$$

Figure 4b suggests that H increased from the outside areas to the middle, indicating the formation of a gradient brush. We are more interested in the relationship between $H(x)$ and $\sigma(x)$. In the low-grafting-density region, H increases only slightly with σ (Figure 4c). Subsequently, a scaling relationship between them with a scaling exponent of 0.15 can be observed. In the even-higher-grafting-density region, the increase in thickness slows down again. We speculate that the absence of pronounced scaling behavior on both sides is

due to the unidirectional extension of the chains. In the region with the highest grafting density, the chains primarily extend towards the low-density region due to the significant compression between chains. The opposite behavior is observed in the low-density region. This explanation is supported by Figure S3. In the high (low)-grafting-density region, the number of monomers consumed by corresponding initiators during polymerization is greater (less) than the actual number of monomers in that region.

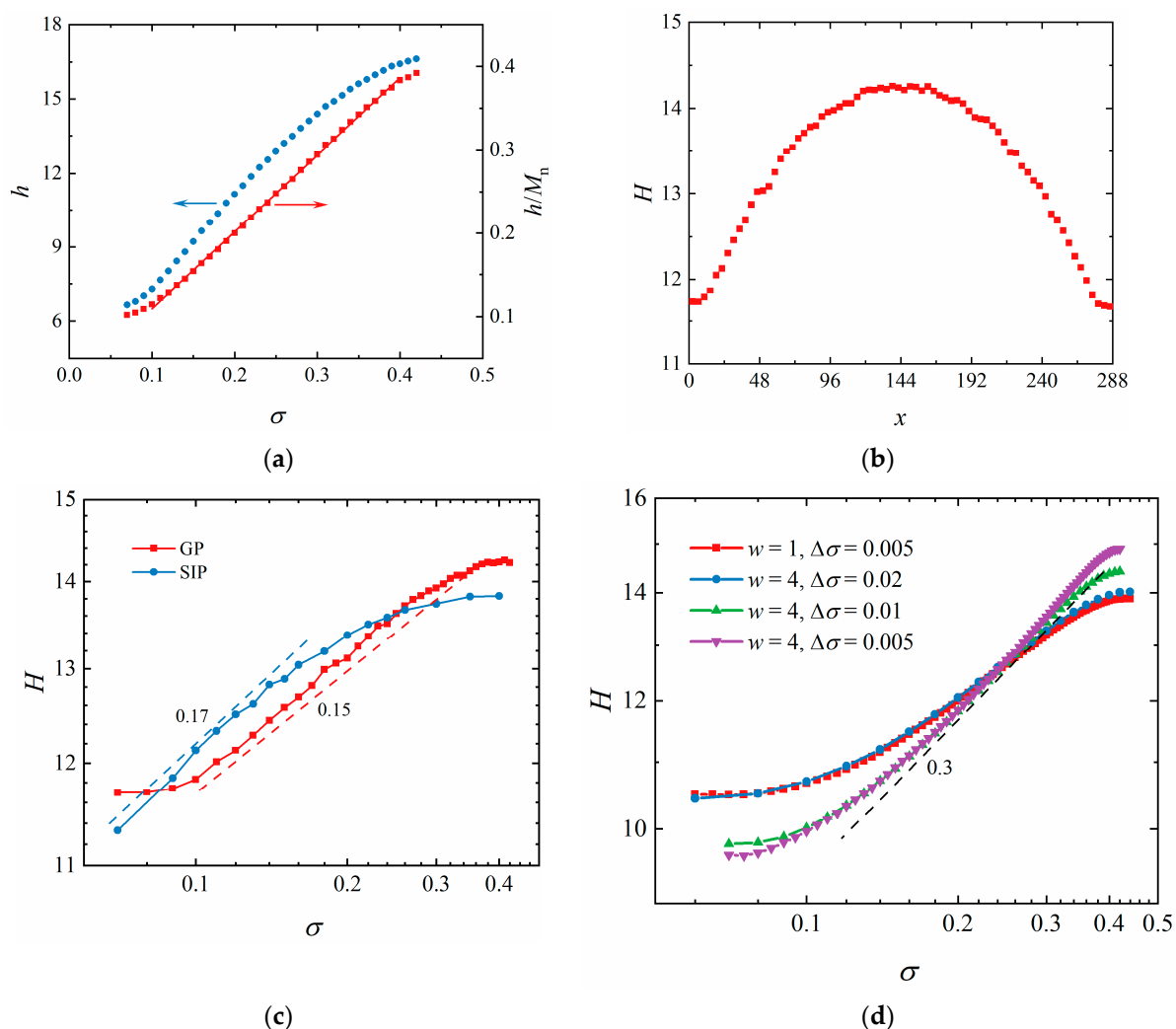


Figure 4. (a) The height of gradient brush in dry state h (circles) and the normalized height h/M_n (squares) as a function of grafting density. (b) The height of gradient brush in solution as a function of position x . (c) The height of gradient polymer brush (square) as a function of grafting density. For comparison, the heights of series polymer brushes formed by surface-initiated polymerization (SIP) at the same reaction time as the gradient polymerization are represented (circles). (d) The effect of steepness on the height of gradient brushes induced by varying the width of the stripes (w) and the difference in grafting density between the adjacent stripes ($\Delta\sigma$). It should be pointed that the gradient brushes shown in (d) are formed by monodisperse polymers for which $M_n = 50$. The slope of the dashed line is 0.3.

If we focus on the scaling behavior in the middle region, the obtained scaling exponent (0.15) is much smaller than both the theoretical value (1/3) [41,42] and the experimental value (0.37–0.4) obtained in Ref. [17]. The theoretical scaling exponent has been extensively validated through simulations [39,43–46], although some simulations suggest that it may not be a constant but instead slightly vary with the grafting density [47]. This raises the

following question: how can we interpret such a smaller scaling exponent obtained in this simulation?

First, the theoretical scaling exponent of one-third was validated for brushes of monodisperse polymers in good solvents. As shown in Figure 3a, in gradient polymerization, M_n decreases with an increasing grafting density in the x direction, and the difference in M_n is significant. Moreover, the polymers at each stripe are polydisperse, and the dispersity increases with the increase in grafting density. Studies have shown that the dispersity of polymers also influences the height of polydisperse polymer brushes [34,48,49]. Thus, in a gradient polymerization system, if we only examine the relationship between height and grafting density, the scaling exponent does not need to adhere to the one-third scaling behavior. We are particularly interested in the experimental value [17], as the non-uniform molecular weight and the dispersity should also be present in the experiment as in this simulation. The fact that the experimental value is close to the theoretical prediction might be related to the method used to calculate the grafting density or instead be a coincidental approximation.

The observed small exponent might relate to the steepness of the initiator gradient. In GBs, polymers experience unbalanced lateral compression in the gradient direction, causing chains in high-grafting-density regions to extend towards regions with lower grafting density. In the experiment, the steepness is negligible as the lateral size of the substrate is 10^6 times larger than the height of the polymer brush [17], while in simulations, the role of steepness should be considered due to the finite simulation size. We can expect that the larger the steepness, the smaller the exponent.

To address this, we studied GBs with different levels of steepness (Figure 4d). It should be pointed out that these GBs consist of polymers with a fixed value of $M_n = 50$, avoiding the influence of non-uniform molecular weight and dispersity observed in gradient polymerization. Figure 4d shows the relationship between brush height and grafting density. When the steepness decreases from 0.005 to 0.0025, the curve exhibits a steeper incline, indicating the influence of steepness. A further reduction in steepness to 0.00125 causes only a minor change in the curve. In this case, the scaling exponent in the middle region is about 0.3, close to the theoretical value. Additionally, we varied the stripe width from $w = 4$ to $w = 1$ while fixing the steepness (Figure 4d), revealing almost identical results. Thus, we believe that the applied steepness is small enough, and this factor is not the main cause of the observed small scaling exponent.

Although the steepness cannot be infinitely small in simulations, we can examine a series of homogeneous SIPs with different initiator densities, the reaction time of which is the same as that of gradient polymerization. This special case allows us to approximate the behavior of gradient brushes with zero steepness. Figure 4c demonstrates that the heights of brushes obtained through SIP display a certain scaling relationship, with a scaling exponent (0.17) slightly larger than that of gradient polymerization (0.15). Thus, we can conclude that the steepness is not the primary cause of the observed small scaling exponent in our simulation.

4. Conclusions

The application of gradient brushes requires critical information regarding properties such as molecular weight and grafting density, which are difficult to characterize experimentally. The assumption that polymers in gradient brushes have uniform properties was commonly adopted in previous experiments, and its validity was questioned but not directly examined. In this study, we employed a stochastic reaction model to investigate surface-initiated polymerization with initiator gradients and analyzed the properties of the resulting gradient brushes.

We first examined surface-initiated polymerizations with homogeneously distributed initiators. The results indicated that, at a given reaction time, polymers with lower molecular weight and higher dispersity were obtained when there was increasing grafting density. This trend can be attributed to the heterogeneous reaction environment inherent in SIP.

Similarly, in SIPs with an initiator gradient, the corresponding polymers exhibited position-dependent properties, with lower molecular weights and higher dispersity at positions with higher grafting density. The difference in molecular weight in gradient brushes, reaching up to 154% (65.5/42.4) in this study, strongly supports the notion that the properties of polymers in gradient brushes are non-uniform.

Subsequent investigation into the height of gradient brushes in solution revealed a small scaling exponent (0.15) in scaling behavior with respect to grafting density, notably deviating from the expected scaling exponent of 1/3. We attributed this discrepancy to the variations in molecular weight and dispersity across space while also excluding the influence of the steepness of initiator gradient. It is noteworthy that a 1/3 scaling exponent is conventionally applied to monodispersed polymer brushes.

We are intrigued by the proximity of the experimental scaling exponent to the theoretical value since the non-uniform properties of polymers should also be present in an experiment. However, we failed to find any other experimental studies of scaling behavior with respect to gradient brushes, and we are uncertain whether this behavior is just a coincidence or if there are underlying mechanisms. It is important to recognize the differences between the simulation and experiments. In the simulation, a living polymerization was modeled, and all initiators reacted, while in the experiment, ATRP was applied [17], and the initiator efficiency was typically low [23].

In summary, this study provides direct evidence of the significant non-uniform properties of polymers in surface-initiated polymerizations with initiator gradients. We hope experimental studies are conducted in the future to better clarify the experimental results in Ref. [17]. Additionally, it would be interesting to investigate surface-initiated polymerizations with other gradients, such as reaction time [13].

Supplementary Materials: The following supporting information can be downloaded at <https://www.mdpi.com/article/10.3390/polym16091203/s1>. Figure S1: Illustration of two possible exchanges between a monomer and a vacancy, which involve bond intersections and are forbidden in this simulation; Figure S2: Illustration of initiators with a homogeneous distribution (left) and a regular distribution (right). Here, the homogeneous distribution means that all initiators are randomly placed on the substrate. While the regular distribution means that initiators are arranged in a certain lattice pattern; Figure S3: In surface-initiated polymerization with initiator gradient, at a given stripe, the number of free monomers consumed by corresponding initiators (red circles), and the number of actual beads of polymers above the stripe (black squares). The former equals the number of chains $N_{\text{chain}}(x)$ multiplied by the corresponding number-average molecular weight $M_n(x)$. While the latter equals the area ($w \times L_z$) multiplied by the corresponding dry height $h(x)$. A smaller number of polymer beads are found in the high grafting regions since the chains tend to extend to lower grafting regions due to the unbalance lateral compression.

Author Contributions: S.J., B.-P.J. and X.-C.S. designed the research and wrote the paper. Z.H., C.G., J.L., P.X. and Y.L. carried out the simulations and analyzed the data. C.G. drew the schematic diagrams. S.J. interpreted the results. All authors have read and agreed to the published version of the manuscript.

Funding: This work was supported by the “Overseas 100 Talents Program” of Guangxi Higher Education, the Natural Science Foundation of China (No. 22263002).

Institutional Review Board Statement: Not applicable.

Data Availability Statement: Data are contained within the article and Supplementary Materials.

Acknowledgments: We thank the reviewer for pointing out the inappropriate expressions used in the manuscript.

Conflicts of Interest: The authors declare no conflicts of interest.

References

1. Lin, X.; He, Q.; Li, J. Complex polymer brush gradients based on nanolithography and surface-initiated polymerization. *Chem. Soc. Rev.* **2012**, *41*, 3584–3593. [[CrossRef](#)]
2. Barbey, R.; Lavanant, L.; Paripovic, D.; Schuwer, N.; Sugnaux, C.; Tugulu, S.; Klok, H.-A. Polymer brushes via surface-initiated controlled radical polymerization: Synthesis, characterization, properties, and applications. *Chem. Rev.* **2009**, *109*, 5437–5527. [[CrossRef](#)]
3. Zhou, X.; Liu, X.; Xie, Z.; Zheng, Z. 3D-patterned polymer brush surfaces. *Nanoscale* **2011**, *3*, 4929–4939. [[CrossRef](#)]
4. Genzer, J. Surface-bound gradients for studies of soft materials behavior. *Annu. Rev. Mater. Res.* **2012**, *42*, 435–468. [[CrossRef](#)]
5. Bhat, R.R.; Tomlinson, M.R.; Wu, T.; Genzer, J. Surface-grafted polymer gradients: Formation, characterization, and applications. *Adv. Polym. Sci.* **2006**, *198*, 51–124.
6. Chen, W.-L.; Cordero, R.; Tran, H.; Ober, C.K. 50th anniversary perspective: Polymer brushes: Novel surfaces for future materials. *Macromolecules* **2017**, *50*, 4089–4113. [[CrossRef](#)]
7. Murad Bhayo, A.; Yang, Y.; He, X. Polymer brushes: Synthesis, characterization, properties and applications. *Prog. Mater. Sci.* **2022**, *130*, 101000. [[CrossRef](#)]
8. Morgenthaler, S.; Zink, C.; Spencer, N.D. Surface-chemical and -morphological gradients. *Soft Matter* **2008**, *4*, 419–434. [[CrossRef](#)]
9. Afzali, Z.; Matsushita, T.; Kogure, A.; Masuda, T.; Azuma, T.; Kushiro, K.; Kasama, T.; Miyake, R.; Takai, M. Cell adhesion and migration on thickness gradient bilayer polymer brush surfaces: Effects of properties of polymeric materials of the underlayer. *ACS Appl. Mater. Interfaces* **2022**, *14*, 2605–2617. [[CrossRef](#)]
10. Kajouri, R.; Theodorakis, P.E.; Deuar, P.; Bennacer, R.; Židek, J.; Egorov, S.A.; Milchev, A. Unidirectional droplet propulsion onto gradient brushes without external energy supply. *Langmuir* **2023**, *39*, 2818–2828. [[CrossRef](#)]
11. Luzinov, I.; Minko, S.; Tsukruk, V.V. Responsive brush layers: From tailored gradients to reversibly assembled nanoparticles. *Soft Matter* **2008**, *4*, 714–725. [[CrossRef](#)] [[PubMed](#)]
12. Tomlinson, M.R.; Efimenko, K.; Genzer, J. Study of kinetics and macroinitiator efficiency in surface-initiated atom-transfer radical polymerization. *Macromolecules* **2006**, *39*, 9049–9056. [[CrossRef](#)]
13. Harris, B.P.; Metters, A.T. Generation and characterization of photopolymerized polymer brush gradients. *Macromolecules* **2006**, *39*, 2764–2772. [[CrossRef](#)]
14. Krabbenborg, S.O.; Huskens, J. Electrochemically generated gradients. *Angew. Chem. Int. Ed.* **2014**, *53*, 9152–9167. [[CrossRef](#)] [[PubMed](#)]
15. Poelma, J.E.; Fors, B.P.; Meyers, G.F.; Kramer, J.W.; Hawker, C.J. Fabrication of complex three-dimensional polymer brush nanostructures through light-mediated living radical polymerization. *Angew. Chem.* **2013**, *125*, 6982–6986. [[CrossRef](#)]
16. Zhang, C.; Wang, L.; Jia, D.; Yan, J.; Li, H. Microfluidically mediated atom-transfer radical polymerization. *Chem. Commun.* **2019**, *55*, 7554–7557. [[CrossRef](#)] [[PubMed](#)]
17. Wu, T.; Efimenko, K.; Genzer, J. Combinatorial study of the mushroom-to-brush crossover in surface anchored polyacrylamide. *J. Am. Chem. Soc.* **2002**, *124*, 9394–9395. [[CrossRef](#)]
18. Liu, Y.; Klep, V.; Zdyrko, B.; Luzinov, I. Synthesis of high-density grafted polymer layers with thickness and grafting density gradients. *Langmuir* **2005**, *21*, 11806–11813. [[CrossRef](#)]
19. Wang, X.; Tu, H.; Braun, P.V.; Bohn, P.W. Length scale heterogeneity in lateral gradients of poly (N-isopropylacrylamide) polymer brushes prepared by surface-initiated atom transfer radical polymerization coupled with in-plane electrochemical potential gradients. *Langmuir* **2006**, *22*, 817–823. [[CrossRef](#)]
20. Coad, B.R.; Bilgic, T.; Klok, H.-A. Polymer brush gradients grafted from plasma-polymerized surfaces. *Langmuir* **2014**, *30*, 8357–8365. [[CrossRef](#)]
21. Sheng, W.; Li, W.; Xu, S.; Du, Y.; Jordan, R. Oxygen-tolerant photografting for surface structuring from microliter volumes. *ACS Macro Lett.* **2023**, *12*, 1100–1105. [[CrossRef](#)]
22. Pester, C.W.; Klok, H.-A.; Benetti, E.M. Opportunities, challenges, and pitfalls in making, characterizing, and understanding polymer brushes. *Macromolecules* **2023**, *56*, 9915–9938. [[CrossRef](#)]
23. Zoppe, J.O.; Ataman, N.C.; Mocny, P.; Wang, J.; Moraes, J.; Klok, H.-A. Surface-initiated controlled radical polymerization: State-of-the-art, opportunities, and challenges in surface and interface engineering with polymer brushes. *Chem. Rev.* **2017**, *117*, 1105–1318. [[CrossRef](#)]
24. Wu, T.; Efimenko, K.; Vlček, P.; Šubr, V.; Genzer, J. Formation and properties of anchored polymers with a gradual variation of grafting densities on flat substrates. *Macromolecules* **2003**, *36*, 2448–2453. [[CrossRef](#)]
25. Genzer, J. In silico polymerization: Computer simulation of controlled radical polymerization in bulk and on flat surfaces. *Macromolecules* **2006**, *39*, 7157–7169. [[CrossRef](#)]
26. Turgman-Cohen, S.; Genzer, J. Computer simulation of concurrent bulk-and surface-initiated living polymerization. *Macromolecules* **2012**, *45*, 2128–2137. [[CrossRef](#)]
27. Liu, H.; Li, M.; Lu, Z.-Y.; Zhang, Z.-G.; Sun, C.-C. Influence of surface-initiated polymerization rate and initiator density on the properties of polymer brushes. *Macromolecules* **2009**, *42*, 2863–2872. [[CrossRef](#)]
28. Xu, J.; Xue, Y.-H.; Cui, F.-C.; Liu, H.; Lu, Z.-Y. Simultaneous polymer chain growth with the coexistence of bulk and surface initiators: Insight from computer simulations. *Phys. Chem. Chem. Phys.* **2018**, *20*, 22576–22584. [[CrossRef](#)]

29. Polanowski, P.; Hałagan, K.; Pietrasik, J.; Jeszka, J.K.; Matyjaszewski, K. Growth of polymer brushes by “grafting from” via ATRP–Monte Carlo simulations. *Polymer* **2017**, *130*, 267–279. [[CrossRef](#)]
30. Xue, Y.-H.; Quan, W.; Liu, X.-L.; Han, C.; Li, H.; Liu, H. Dependence of grafted polymer property on the initiator site distribution in surface-initiated polymerization: A computer simulation study. *Macromolecules* **2017**, *50*, 6482–6488. [[CrossRef](#)]
31. Arraez, F.J.; Van Steenberge, P.H.M.; Sobieski, J.; Matyjaszewski, K.; D’hooge, D.R. Conformational variations for surface-initiated reversible deactivation radical polymerization: From flat to curved nanoparticle surfaces. *Macromolecules* **2021**, *54*, 8270–8288. [[CrossRef](#)]
32. Arraez, F.J.; Van Steenberge, P.H.; D’hooge, D.R. The competition of termination and shielding to evaluate the success of surface-initiated reversible deactivation radical polymerization. *Polymers* **2020**, *12*, 1409. [[CrossRef](#)]
33. Li, W. Molecular dynamics simulations of ideal living polymerization: Terminal model and kinetic aspects. *J. Phys. Chem. B* **2023**, *127*, 7624–7635. [[CrossRef](#)]
34. Yang, B.; Liu, S.; Ma, J.; Yang, Y.; Li, J.; Jiang, B.-P.; Ji, S.; Shen, X.-C. A Monte Carlo simulation of surface-initiated polymerization: Heterogeneous reaction environment. *Macromolecules* **2022**, *55*, 1970–1980. [[CrossRef](#)]
35. Ma, J.-S.; Huang, Z.-N.; Li, J.-H.; Jiang, B.-P.; Liao, Y.-D.; Ji, S.-C.; Shen, X.-C. Simultaneous bulk- and surface-initiated living polymerization studied with a heterogeneous stochastic reaction model. *Chin. J. Polym. Sci.* **2023**, *42*, 364–372. [[CrossRef](#)]
36. Ma, J.; Li, J.; Yang, B.; Liu, S.; Jiang, B.-P.; Ji, S.; Shen, X.-C. A simple stochastic reaction model for heterogeneous polymerizations. *Polymers* **2022**, *14*, 3269. [[CrossRef](#)]
37. Larson, R. Monte Carlo lattice simulation of amphiphilic systems in two and three dimensions. *J. Chem. Phys.* **1988**, *89*, 1642–1650. [[CrossRef](#)]
38. Larson, R.; Scriven, L.; Davis, H. Monte Carlo simulation of model amphiphile-oil-water systems. *J. Chem. Phys.* **1985**, *83*, 2411–2420. [[CrossRef](#)]
39. Ji, S.; Ding, J. Rheology of polymer brush under oscillatory shear flow studied by nonequilibrium Monte Carlo simulation. *J. Chem. Phys.* **2005**, *123*, 144904. [[CrossRef](#)] [[PubMed](#)]
40. Farah, K.; Müller-Plathe, F.; Böhm, M.C. Classical reactive molecular dynamics implementations: State of the art. *ChemPhysChem* **2012**, *13*, 1127–1151. [[CrossRef](#)] [[PubMed](#)]
41. de Gennes, P.G. Conformations of polymers attached to an interface. *Macromolecules* **1980**, *13*, 1069–1075. [[CrossRef](#)]
42. Milner, S.T.; Witten, T.A.; Cates, M.E. Theory of the grafted polymer brush. *Macromolecules* **1988**, *21*, 2610–2619. [[CrossRef](#)]
43. Murat, M.; Grest, G.S. Structure of a grafted polymer brush: A molecular dynamics simulation. *Macromolecules* **1989**, *22*, 4054–4059. [[CrossRef](#)]
44. Jehser, M.; Zifferer, G.; Likos, C.N. Scaling and interactions of linear and ring polymer brushes via DPD simulations. *Polymers* **2019**, *11*, 541. [[CrossRef](#)]
45. Binder, K.; Milchev, A. Polymer brushes on flat and curved surfaces: How computer simulations can help to test theories and to interpret experiments. *J. Polym. Sci. Part B Polym. Phys.* **2012**, *50*, 1515–1555. [[CrossRef](#)]
46. Polanowski, P.; Sikorski, A. The structure of polymer brushes: The transition from dilute to dense systems: A computer simulation study. *Soft Matter* **2021**, *17*, 10516–10526. [[CrossRef](#)]
47. Whitmore, M.D.; Grest, G.S.; Douglas, J.F.; Kent, M.S.; Suo, T. End-anchored polymers in good solvents from the single chain limit to high anchoring densities. *J. Chem. Phys.* **2016**, *145*, 174904. [[CrossRef](#)]
48. Milner, S.T.; Witten, T.A.; Cates, M.E. Effects of polydispersity in the end-grafted polymer brush. *Macromolecules* **1989**, *22*, 853–861. [[CrossRef](#)]
49. Qi, S.; Klushin, L.I.; Skvortsov, A.M.; Schmid, F. Polydisperse polymer brushes: Internal structure, critical behavior, and interaction with flow. *Macromolecules* **2016**, *49*, 9665–9683. [[CrossRef](#)]

Disclaimer/Publisher’s Note: The statements, opinions and data contained in all publications are solely those of the individual author(s) and contributor(s) and not of MDPI and/or the editor(s). MDPI and/or the editor(s) disclaim responsibility for any injury to people or property resulting from any ideas, methods, instructions or products referred to in the content.